



Biologically inspired collective construction with visual landmarks*

Zheng-wei ZHANG^{†1}, Hong ZHANG^{†2}, Yi-bin LI¹

(¹School of Control Science and Engineering, Shandong University, Jinan 250061, China)

(²Department of Computing Science, University of Alberta, Edmonton, Alberta T6G 2E8, Canada)

[†]E-mail: zzwwei21cn@mail.sdu.edu.cn; hzhang@ualberta.ca

Received Aug. 22, 2011; Revision accepted Feb. 14, 2012; Crosschecked Apr. 9, 2012

Abstract: We describe our research in using environmental visual landmarks as the basis for completing simple robot construction tasks. Inspired by honeybee visual navigation behavior, a visual template mechanism is proposed in which a natural landmark serves as a visual reference or template for distance determination as well as for navigation during collective construction. To validate our proposed mechanism, a wall construction problem is investigated and a minimalist solution is given. Experimental results show that, using the mechanism of a visual template, a collective robotic system can successfully build the desired structure in a decentralized fashion using only local sensing and no direct communication. In addition, a particular variable, which defines tolerance for alignment of the structure, is found to impact the system performance. By decreasing the value of the variable, system performance is improved at the expense of a longer construction time. The visual template mechanism is appealing in that it can use a reference point or salient object in a natural environment that is new or unexplored and it could be adapted to facilitate more complicated building tasks.

Key words: Biologically inspired, Swarm robotics, Collective construction, Visual landmark, Template

doi:10.1631/jzus.C1100243

Document code: A

CLC number: TP242

1 Introduction

Imagine a scenario where a natural disaster, such as an earthquake, occurs and rescuers release swarms of building robots that could collectively and cooperatively build homes for people. This is one possible application of a multi-robot swarm that could be envisioned. Other applications include construction under extreme physical conditions. For example, robots could perform construction undersea withstanding high pressures, in extreme temperature environments or in oxygen deficient outer space, etc., where human presence is not conducive, expensive, or even impossible (Skibniewski, 2000; Wawerla *et al.*, 2002; Parker and Zhang, 2006; Stewart and

Russell, 2006; Werfel *et al.*, 2006). In such environments, construction by autonomous robots might be the only viable alternative.

Swarm robotics has drawn increasing attention over the last decade and great achievements have been made (Payton *et al.*, 2005; Bayindir and Sahin, 2009; Purnamadajaja and Russell, 2010; Berman *et al.*, 2011; Parker and Zhang, 2011). In this paper, we focus on one problem domain in swarm robotics, that is, collective construction which is concerned with the building of a geometric structure with a collection of robots working in parallel, without centralized control (Kube *et al.*, 2005). Some researchers in this field focus on the robot design (Terada and Murata, 2004), but the primary goal of this paper is to study the feasibility of the proposed mechanism. Several mechanisms have already been proposed, including stigmergic (Kelly and Zhang, 2006),

* Project (No. 61075091) supported by the National Natural Science Foundation of China

blind-bulldozing (Parker *et al.*, 2003), pheromone-based (Ladley and Bullock, 2005), and blueprint-based (Werfel and Nagpal, 2008) methods. In this paper, we propose a visual template method. The inspiration comes from the observation of social insects. These insects, such as termites, ants, wasps, and bees, employ templates (patterns) in the environment to organize and coordinate their building activities (Bonabeau *et al.*, 1998; Camazine *et al.*, 2001). A template can be defined as a heterogeneity (e.g., taking the form of a chemical, humidity, temperature, or light heterogeneity) which is a perceptible (by the insects) deviation from a uniform distribution or constant quantity (Theraulaz *et al.*, 1998; 2003).

The notion of employing a template in collective construction is not, in itself, novel. Melhuish *et al.* (1999) derived inspiration from ants using two templates in the environment to build linear wall structures. The first template was a strip of white tape preplaced across the arena. When detecting the white tape, robots were stimulated to deposit building materials at a certain distance from it. To achieve orientation, robots employed a second template consisting of a bank of halogen lights at one side of the arena. Although the mechanisms involved are very simple, these predeployed templates are highly restrictive and prevent operations in a new or unexplored environment. Stewart and Russell (2006) proposed another method for construction. There was a leader robot in the system emitting a light beam that served as a light-field template to the construction robots. Robots could build more complicated structures when this leading robot moved in a predefined pattern. However, relying on an artificial template would restrict the robustness of the system. The loss of the organizer robot implies the loss of the template.

Wawerla *et al.* (2002) have also demonstrated linear wall construction. Equipped with a color camera, each robot could find a block and then carry it to the construction site using a laser range finder. Robots could build an approximately continuous barrier out of cardboard blocks. However, the blocks in their work had to be labelled differently to be distinguished and robots would need to communicate with each other to coordinate their building process.

The visual template mechanism proposed in this

paper derives its origin from honeybee visual navigation behavior. More importantly, this visual template mechanism can use an interesting landmark, reference point, or salient object in the construction environment. This approach is more natural, easier to implement and also more robust for the system than the artificial counterpart. Furthermore, the visual template mechanism allows for robots manipulating homogeneous bricks in a non-communicative way. Such a mechanism has an obvious appeal to those researching collective construction for applications in unknown environments. The aim of this paper is specifically to study the feasibility of the proposed mechanism by focusing on the problem of linear wall construction in a planar, bounded environment. To our knowledge, this is the first time that a visual template mechanism has been used in collective construction.

2 Background and motivation

The motivation for the study comes from observations that honeybees use visual features during their approach to the desired goal (Collett and Collett, 2002; Collett *et al.*, 2003). Specifically, honeybees use the azimuthal retinal position of the landmark as a visual cue for navigation (Fry and Wehner, 2005). Inspired by the honeybee's simple and elegant navigation behavior, we wonder whether a visual landmark could be used in collective construction. The aim of this paper is specifically to study the feasibility of the proposed method.

3 Visual template

The purpose of the visual template mechanism is to construct a physical structure with the help of a visual landmark. The visual template mechanism serves two purposes: reaching the construction zone location and localizing the construction sites within the zone. As shown in Fig. 1, to make progress in construction, the robots first move to the construction zone and position themselves within the construction zone at the construction sites, before executing a fixed motion sequence for the deposition of construction materials. In the following two subsections, we will discuss the visual template mechanism in detail. Note that we use the terms 'landmark' and 'beacon' interchangeably in this paper.

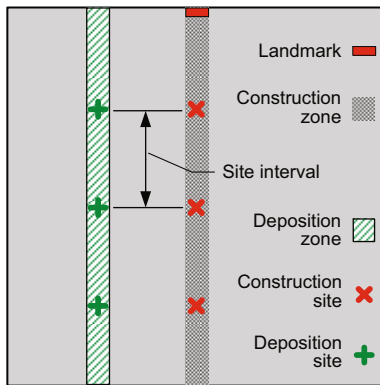


Fig. 1 A schematic diagram of the environment setup. The construction zone is located right in front of the landmark and the deposition zone is to the left of the construction zone

3.1 Visual navigation to construction zone

Analogous to a honeybee's use of the azimuthal retinal position of a landmark, our vision-based robots use the horizontal position of the landmark in an image to navigate. Construction robots with a frontal landmark ignore the laterally moving landmark when they move. It is only when the landmark is at the periphery of the robot's visual field that a compensatory turning reacts.

As shown in Fig. 2, a robot at any location *A*, can move to the construction zone by first rotating about its center until the landmark lies in the middle of the robot's visual field, then assessing whether it has entered the construction zone. If not, the robot makes a move in a circular arc until the landmark is at the periphery of the robot's visual field to arrive at location *B*. The turning direction depends on the relative position of the robot with respect to the landmark. If the robot is on the left-hand side of the construction zone, the robot turns clockwise in an arc; otherwise, it turns counter-clockwise. Then the robot repeats the above steps until it is aligned directly in front of the landmark, i.e., in the construction zone.

This sequence of actions is referred to as a 'look-and-turn navigation behavior'. The design of this navigation behavior has four considerations: firstly, the robotic swarm should consist of some relatively simple robots and collective construction be achieved without recourse to direct communication, sophisticated sensing, or intensive computation; secondly, the visual landmark used for navigation should always lie within the robot's visual field; thirdly, the

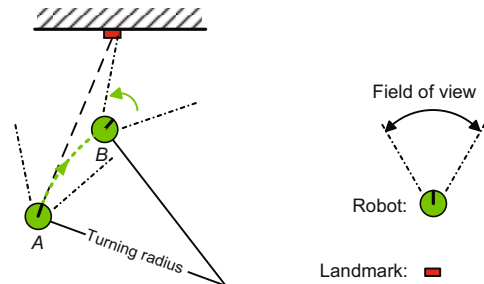


Fig. 2 A look-and-turn visual navigation strategy. A robot at location *A* firstly rotates about its center until the landmark lies in the middle of the robot's visual field, and then makes a circular move until the landmark is at the periphery of the robot's visual field to arrive at location *B*. See more details in the text

navigation behavior should allow the robots to arrive at the construction zone; fourthly, on arrival at the construction zone, the further the distance of robots to the landmark, the better—This is because a further distance means robots are more likely to find a construction site and thus generally increases the success rate for deposition. The first two considerations are constraints that emphasize the limitations in the individual capabilities relative to the task and these constraints ensure that the study falls within the swarm robotics research. The last two considerations are the purposes that the visual navigation behavior should accomplish.

In the simulation and physical experiments section, we will present the choice of a proper turning radius and demonstrate that the proposed navigation behavior will cause the robots to navigate to the construction zone.

3.2 Visual localization

Once inside the construction zone, robots are required to reach construction sites before executing the deposition behavior. Construction sites in our experiments are locations that are evenly spaced within the zone front of the landmark (Fig. 1). When robots are inside the construction zone, the problem of reaching the construction sites becomes easy to deal with. Since the length of an object in a robot's camera image plane is related to the inverse of the distance between the robot and the object (Hartley and Zisserman, 2004), we can use this information to determine the distance of a robot to the landmark.

4 Linear wall construction

In the previous section, we introduced our visual template mechanism. In this section, we will describe a linear wall construction task followed by a minimalist behavior-based solution.

4.1 Task description

Robots are required to build a linear wall structure out of identical square bricks. No direct communication exists among construction robots and these robots rely on their local sensing capabilities to determine the state of the environment and the progress of the task. In the system, the camera on each robot serves as the sensor pointing in the direction of the robot's heading. Due to the relatively small experimental arena, it is assumed that all the objects that are within the field of view of a robot can be detected.

4.2 The controller

The behavior of construction robots can be implemented in the form of a finite state machine. A six-state finite state machine implementation for the robots' controller is given in Fig. 3 and in each of the six states, a robot is controlled by a behavior-based controller. Transition between states is triggered by sensory events (Kube and Zhang, 1993). In particular, two of the states, GoToBeacon and GoToSite, require the use of the visual landmark already described in the previous section. The other four states also use visual data observed by the robot's camera, although they do not rely on the visual landmark.

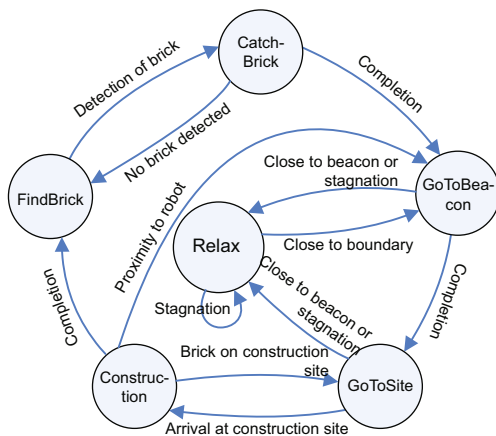


Fig. 3 A six-state finite state machine implementation of the wall construction algorithm

1. FindBrick: Robots enter this state both at the beginning of the experiment and when they finish one-brick deposition. In this state, robots look for construction materials, i.e., bricks, with the help of a camera. To do this, robots continuously detect the environment while rotating back and forth for a certain degree. This behavior ensures robots do not handle bricks already deposited. When an obstacle is detected in the immediate vicinity, robots stop rotating and wait until the obstacle moves away. Here an obstacle refers to another robot. Upon detection of bricks, robots switch to the CatchBrick state.

2. CatchBrick: This state moves a robot to a detected brick to pick it up. While moving towards the brick, the detection of other robots in an immediate vicinity causes the robot to wait until the obstacle moves away. This ensures robots do not turn away to handle bricks that have already been deposited. Due to the lack of centralized control, it is possible for a brick to be detected by two or more robots, and the late arrival robots will make transitions back to the FindBrick state as a result. Once a robot picks up a brick, it switches to the GoToBeacon state.

3. GoToBeacon: The behavior of the robot in this state is guided by the visual landmark described in the previous section, with the additional consideration that upon detection of any obstacle in the immediate vicinity, robots stop executing the look-and-turn behavior and then turn away from the obstacle. When the obstacle is no longer visible in the immediate vicinity, robots continue to execute the look-and-turn behavior. Once inside the construction zone, robots switch their state to GoToSite. This behavior does not always succeed in guiding the robot to the construction zone, and in case of failure, the robot enters the error recovery behavior (the behavior in the Relax state) to resolve the failure cases to some extent.

4. GoToSite: Once again, the behavior of the robots in this state is guided by the visual landmark defined in the previous section. Robots are pre-programmed to know the distance from each construction site to the landmark. While in this state, the robots avoid obstacles by stopping their motion. Once a robot arrives at a construction site, it enters the Construction state.

5. Construction: A robot in this state is at a construction site while holding a brick. It will execute a fixed motion before depositing the brick in its

possession. As shown in Fig. 1, the deposition sites are within the deposition zone and are parallel to the construction sites. To reach a deposition site from a construction site, a robot has three steps to follow: it first makes a counter-clockwise rotation of 90° , then moves straight ahead for a fixed distance, and finally puts down its brick by reversing and then performing a 180° turn to finish one brick deposition process. Only one brick can be deposited at each deposition site; therefore, robots always check the state of deposition sites before implementing the second step. If a deposition site is occupied by a brick, the robot will rotate itself 90° clockwise, and then switch back to the GoToSite state to try another construction site. If a robot encounters another robot when moving towards the deposition site, it stops moving and switches back to the GoToBeacon state.

6. Relax: During the states of GoToBeacon and GoToSite, when a robot gets too close to the beacon (landmark) or experiences deadlock (where a watchdog timer triggers a system reset because the robot has stagnated in position for more than a certain time), it will enter the Relax state, in which the robot rotates and then travels straight until it reaches the boundary of the experimental environment. The rotation angle depends on the trigger for the state transition. If the trigger is the proximity, the rotation angle is set to 180° . Otherwise, the robot makes a random turn. The robot avoids any obstacle by changing its heading in response. The proximity to the boundary of the experimental arena drives the robot back to the GoToBeacon state.

5 Experimental design

To validate our approach, we performed both simulation and physical experiments. For the simulation part, we first analyzed the look-and-turn walking strategy to determine a reasonable turning radius. Secondly, we were able to show that with the controller described in Section 4, simulated robots can collectively build a wall structure. For the physical part, we conducted experiments using one and two physical robots, respectively, to investigate the performance of the same controller and to explore the factors influencing the system performance. Each robot had an odometry sensor, which was necessary in our experiments. Our robots performed object detection and obstacle avoidance by means of simple

color vision.

At the beginning of the experiments, bricks were placed randomly on one side of the arena. Robots had no explicit global knowledge about their own locations, the positions of the bricks, or the location of the beacon; instead, they moved under the guidance of the beacon.

5.1 Simulation

The simulation was performed in Matlab, and conducted in a planar bounded environment, $4\text{ m} \times 4\text{ m}$ in size, with a beacon located in the middle of one boundary wall.

Two sets of simulation were designed. In the first set, we demonstrated the effectiveness of the look-and-turn walking pattern in terms of navigation and then analyzed the performances with different turning radii. In the second set, the performances of the controller with different system populations were measured. In both cases, robots had a field of view (FOV) of 55° , as in the case with real robots.

When analyzing the performance with different turning radii, we studied the navigation path that the robot moves along. The navigation path consists of segments of circular arcs with the end of each arc being the start of the next one. For one circular arc from a starting point A to an end point B in Fig. 4, we can derive the formula

$$(x - o_{ix})^2 + (y - o_{iy})^2 = r^2, \quad (1)$$

where $x_i \leq x \leq x_{i+1}$, $y_i \leq y \leq y_{i+1}$, $\alpha = \text{FOV}/2$. The variables d_i , o_{ix} , o_{iy} , φ_i , t_i , θ_i , β_i , x_{i+1} , and y_{i+1} can be expressed as

$$d_i = \sqrt{(x_i - a_0)^2 + (y_i - b_0)^2}, \quad (2)$$

$$o_{ix} = x_i + \frac{r(b_0 - y_i)}{d_i}, \quad (3)$$

$$o_{iy} = y_i - \frac{r(a_0 - x_i)}{d_i}, \quad (4)$$

$$\varphi_i = \arctan(r/d_i), \quad (5)$$

$$t_i = \sqrt{r^2 \sin^2 \alpha + d_i^2} - r \sin \alpha, \quad (6)$$

$$\theta_i = \arccos \frac{d_i^2 + t_i^2}{2t_i \sqrt{r^2 + d_i^2}}, \quad (7)$$

$$\beta_i = \alpha - (\varphi_i - \theta_i), \quad (8)$$

$$x_{i+1} = o_{ix} + r \cos \left(\arctan \frac{y_i - o_{iy}}{x_i - o_{ix}} - \beta_i \right), \quad (9)$$

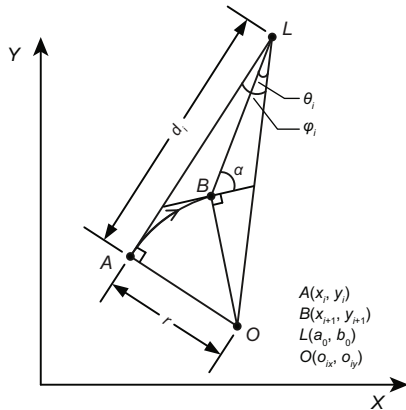


Fig. 4 Geometrical analysis of the visual navigation path. The robot at location $A(x_i, y_i)$ first rotates about its center until the landmark L lies in the middle of the robot's visual field, and then makes a move in a circular arc of radius r until the landmark is at the periphery of the robot's visual field to arrive at location $B(x_{i+1}, y_{i+1})$. The angle α is half of the field of view (FOV) of the robot

$$y_{i+1} = o_{iy} + r \sin \left(\arctan \frac{y_i - o_{iy}}{x_i - o_{ix}} - \beta_i \right). \quad (10)$$

Based on the geometric constraint that the end of one arc is the start of the next, we can determine the navigation path by iteratively calculating Eqs. (1)–(10). The navigation path ends when the x -coordinate of the path reaches a_0 . This means the robot reaches the construction zone (hereafter we call the end point of the path 'entry point').

In the second set of simulation, bricks were represented by $0.15 \text{ m} \times 0.15 \text{ m}$ rectangles. Building robots had a circular shape and the same size as actual robots in our physical experiments with a diameter of 0.33 m . The robot body would change its color once it picked up a brick so that users could easily distinguish those robots carrying bricks from those that are not. The space interval between neighboring deposition sites was 0.4 m , and there were nine deposition sites in total. We defined the completion of the linear wall building task to be when all the nine deposition sites were occupied by bricks.

5.2 Physical experiments

We used iRobot Roomba 400 robots, each equipped with an AXIS network camera and a RoBoDynamics RooTooth bluetooth module, in our experiments. A Roomba robot cannot pick up bricks; it instead depends on pushing to manipulate a brick around the environment (Fig. 5).

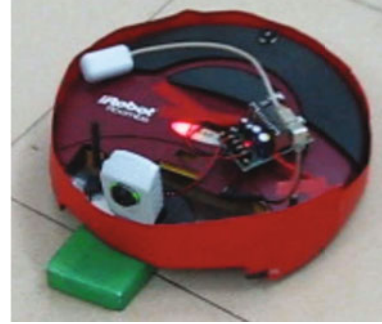


Fig. 5 Close-up view of a construction robot used in the wall construction experiments. We used iRobot Roomba 400 robots as our construction robots. The robot cannot pick up the brick (cardboard in the bottom left of the figure), but a similar level of functionality can be achieved by pushing the brick around the floor

The physical environment was rectangular, $2.09 \text{ m} \times 2.02 \text{ m}$ in size, with the beacon located in the middle of one boundary wall. For experimental convenience, bricks, robots, and the beacon were colored differently to facilitate detection: bricks were represented by green cardboard blocks, robots had a strip of red tape attached around their perimeter, and the beacon was represented by a landmark of two horizontally aligned circles of equal size. A simple thresholding algorithm for image segmentation was adequate for detection of the bricks, the beacon, and the robots. After a simple thresholding-based segmentation of the current view, robots performed centroid detection to determine the horizontal position of the object of interest in the image and measured the segmented area in pixels to determine the size of the object. Fig. 6 shows three filtered images using this method.

In our physical experiments, the process of evaluating whether the alignment of the robot and the

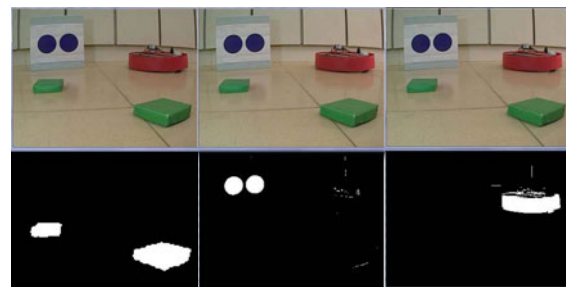


Fig. 6 Filtered images of different objects (from left to right: two bricks, the landmark of two horizontally aligned circles of equal size, and the construction robot). Objects were segmented using a simple thresholding algorithm

beacon was achieved was implemented through the comparison of two parameters: q and q_0 , where $q = |S_1 - S_2|/(S_1 + S_2)$, S_1 and S_2 are the image sizes of the two circles, and q_0 is a preset threshold value which corresponds to an allowed maximum value of q . When $q \leq q_0$, robots were assumed to be within the construction zone where the alignment with the beacon was achieved.

When the robot is within the construction zone, the relationship between the distance to the beacon d and the size of the beacon in pixels in the robot's image S can be approximated by (Hartley and Zisserman, 2004)

$$d = \sqrt{\frac{S_D \cdot D^2}{S}}, \quad (11)$$

where D is a predefined constant and S_D is the size of the beacon in pixels in the image when the robot is at a distance of D away from the beacon with its heading aligned with the beacon. Since we used a landmark of two circles to represent the beacon, we assumed $S = (S_1 + S_2)/2$.

The aim of these experiments is to verify the viability of the visual template mechanism in building a wall structure, investigate the performance of the same controller, and explore the factors influencing system performance. In the physical experiments, for performance evaluation, we defined success as the deposition of at least three bricks.

6 Results and discussion

6.1 Simulation

6.1.1 Look-and-turn

Considering that the longest turning radius of a physical robot is 2 m, we chose the radius values of 0.2 m, 0.5 m, 1 m, and 2 m in simulation. Four trials with the four different radii were conducted. During each trial, 12 positions on one side of the experimental environment (black squares in Fig. 7) were selected as the starting points from which robots started the GoToBeacon behavior. The recorded trajectories are shown in Figs. 7a–7d.

Fig. 7 shows that our look-and-turn walking strategy allows the robots to move to the construction zone. Due to symmetry, similar results would be expected for right-hand side starting points.

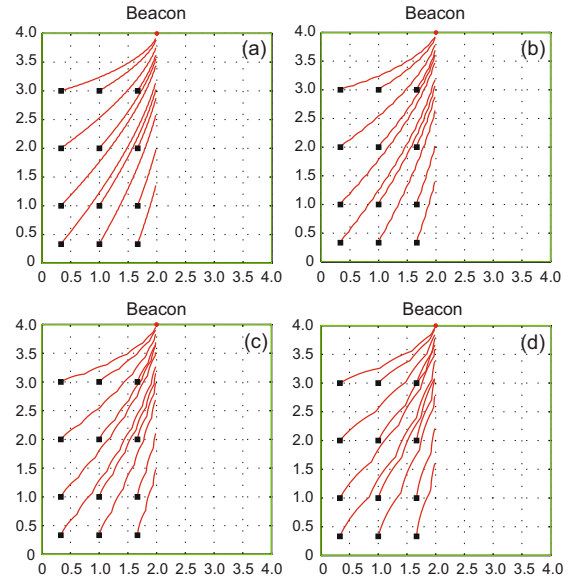


Fig. 7 The trajectories of robots with different turning radii (TR) in the 4 m × 4 m planar bounded environment. Lines indicate trajectories of robots starting from 12 different starting points (black squares). (a) TR = 0.2 m; (b) TR = 0.5 m; (c) TR = 1 m; (d) TR = 2 m

To select a reasonable turning radius value, we studied the performance with different turning radii. That is, we analyzed the navigation path by fixing the starting point position and varying the turning radii. We used three metrics to gauge the performance. The first metric, which we call the ‘path length’, is the length of the navigation path. The second metric, the number of arcs, tells us the number of circular arcs that the navigation path consists of. Since robots check the alignment with the landmark where neighboring arcs intersect, the number of arcs equals the number of checks. Ultimately, what we desire is a further distance of the entry point to the landmark. Thus, we used the distance of the entry point to the landmark as the third metric.

Results are shown in Figs. 8–10. These graphs plot the path length, number of arcs, and distance of the entry point to the landmark versus different turning radii. Given a starting point, the navigation length and the distance of the entry point to the landmark were not sensitive to the turning radius. Furthermore, a smaller radius means the robot checks more often which is desirable; on the other hand, with a smaller radius, the robot will have to stop and rotate more frequently. We made a trade-off and chose the radius value of 0.2 m. This value

will be used in the subsequent experiments.

6.1.2 Collective wall construction

Simulation was performed with one, two, four, six, and eight robots, respectively. Each set underwent 20 trials. To prevent extremely long simulation time, simulation was limited to running 100 000 loops.

Fig. 11 shows representative snapshots during the process of wall construction with two robots. The results with different numbers of robots are summarized in Fig. 12 and Table 1. The mean construction time μ decreased up until six robots and increased for eight robots. For all population sizes, construction progressed quickly in the beginning, with the last bricks of the wall taking a significant amount of time, as each subsequent brick requires more time for the robot(s) to find a vacant spot for it. Furthermore, the progress vs. time can be approximately described as a decaying exponential of the form $p(t) = 1 - \exp(-t/\tau)$. The differences between different progress curves would be in the rates of exponential decay (the value of τ). We used the least squares approach to fit the decaying exponential function to the experimental data. The 63% completion times for 1 to 8 robots are listed in Table 2 together with the τ values when the data was fitted to the exponential decay curves.

Note that the overall building rates for four robots and eight robots are similar. The reason is the overcrowding in the environment. Fig. 7 shows that the proposed visual template mechanism is biased for locations closer to the beacon. This makes the robots converge to a relatively small area and interference often takes place. The situation worsens if there are more robots in the environment. By enlarging the size of the environment or by broadening the robots' field of view, an improvement of the system performance would be expected. Since the larger the environment size, the less the interference, and the wider the field of view, the more robots will navigate to the construction zone locations that are further away from the beacon.

6.2 Physical experiments

6.2.1 One-robot case

Figs. 13 and 14 show a sequence of images taken during two experimental trials with different

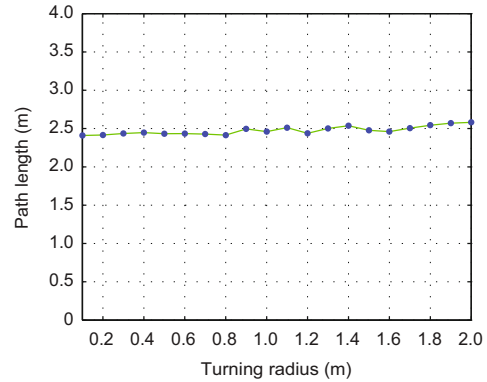


Fig. 8 The length of the navigation path with turning radius values ranging from 0.1 m to 2.0 m. Results were obtained through iteratively calculating Eqs. (1)–(10). The starting point is at (1, 1), the landmark at (2, 4), and $\alpha = 27.5^\circ$

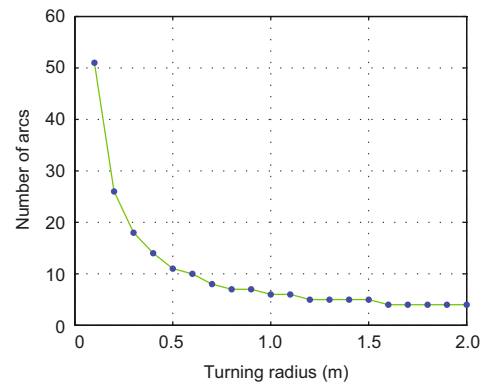


Fig. 9 The number of circular arcs that the navigation path consists of with turning radius values ranging from 0.1 m to 2.0 m. Results were obtained through iteratively calculating Eqs. (1)–(10). The starting point is at (1, 1), the landmark at (2, 4), and $\alpha = 27.5^\circ$

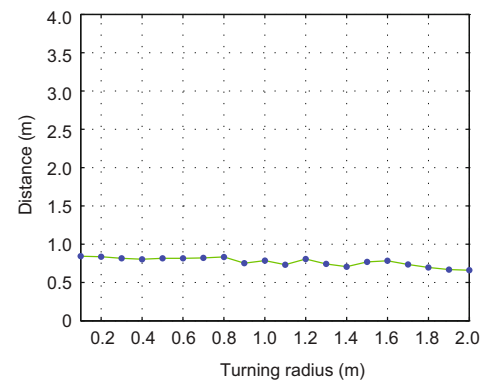


Fig. 10 The distance between the landmark and the entry point with turning radius values ranging from 0.1 m to 2.0 m. Results were obtained through iteratively calculating Eqs. (1)–(10). The starting point is at (1, 1), the landmark at (2, 4), and $\alpha = 27.5^\circ$

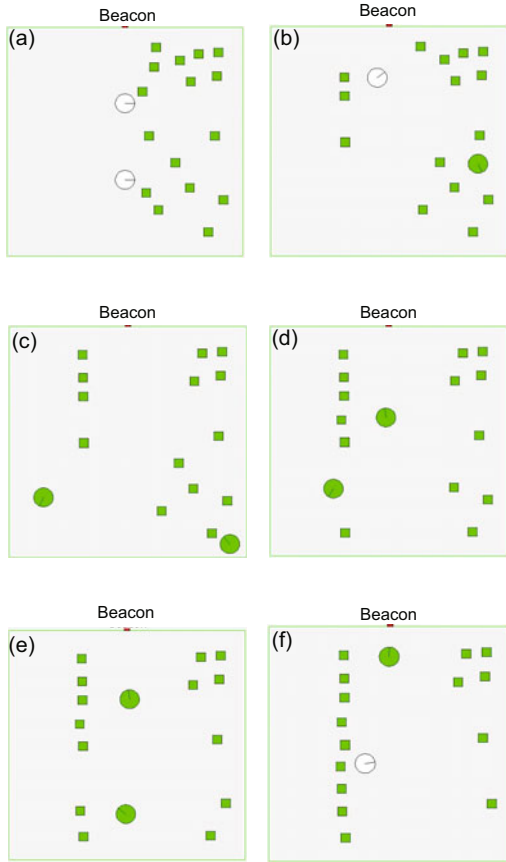


Fig. 11 Linear wall construction with two robots in a 4 m \times 4 m environment. Robots that are carrying bricks are indicated by colored circles and robots that are not carrying bricks with white circles. Bricks are indicated by colored squares, and are initially randomly placed on the right side of the environment. The beacon is indicated by a rectangle located in the middle of a boundary wall. (a) Time step = 0; (b) Time step = 500; (c) Time step = 2000; (d) Time step = 4000; (e) Time step = 5000; (f) Time step = 5720

q_0 values. The results demonstrate that using the proposed visual template mechanism the robot succeeded in the wall construction task. From Figs. 13f and 14f, we can see that the first brick which is the closest to the beacon is deposited very close to the desired deposition site and the following ones have an offset in their position due to the inaccuracy in finding the construction sites. The parameters of q and q_0 determine the accuracy in finding the construction zone. A decrease in the value of q_0 can reduce the deposition inaccuracy (Fig. 14). However, the results suggest that under such conditions robots take more time in completing the task, 586 s vs. 443 s. Another factor influencing the performance of depo-

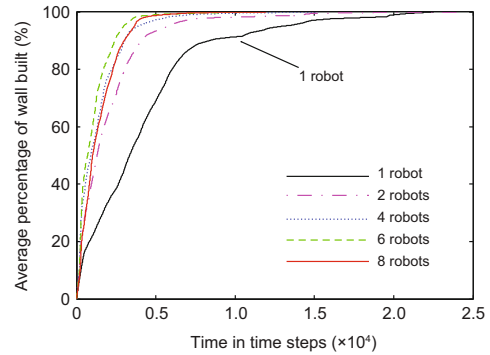


Fig. 12 Average percentage of wall built through time for different system populations

Table 1 Means and standard deviations of construction time for different population sizes

Number of robots	μ (time step)	σ
1	9207	4460
2	7768	6174
4	5243	3150
6	3835	2248
8	4299	2249

μ : mean of construction time; σ : standard deviation of construction time

Table 2 Results for the progress curves

Number of robots	λ (time step)	τ
1	4422	4195
2	1931	1878
4	1396	1324
6	1102	1034
8	1519	1422

λ : time required for the construction process to reach 63% completion; τ : exponential decay rate of the fitting curve

sition is noise. Since sensors are noisy, and the length of an object in the robot's camera image plane is related to the inverse of the distance between the robot and the object, when robots are far from the beacon, the corresponding size of the beacon image is small. In such situations, the noise of the image plays a more important role and eventually gives rise to the inaccuracy of deposition location.

6.2.2 Two-robot case

Experimental results shown in Fig. 15 demonstrate that our controller works in a decentralized fashion using only local sensing and no direct communication. Furthermore, using the visual template mechanism, robots can collectively accomplish the construction task faster: 338 s for the two-robot case vs. 586 s for the one-robot case, which is consistent

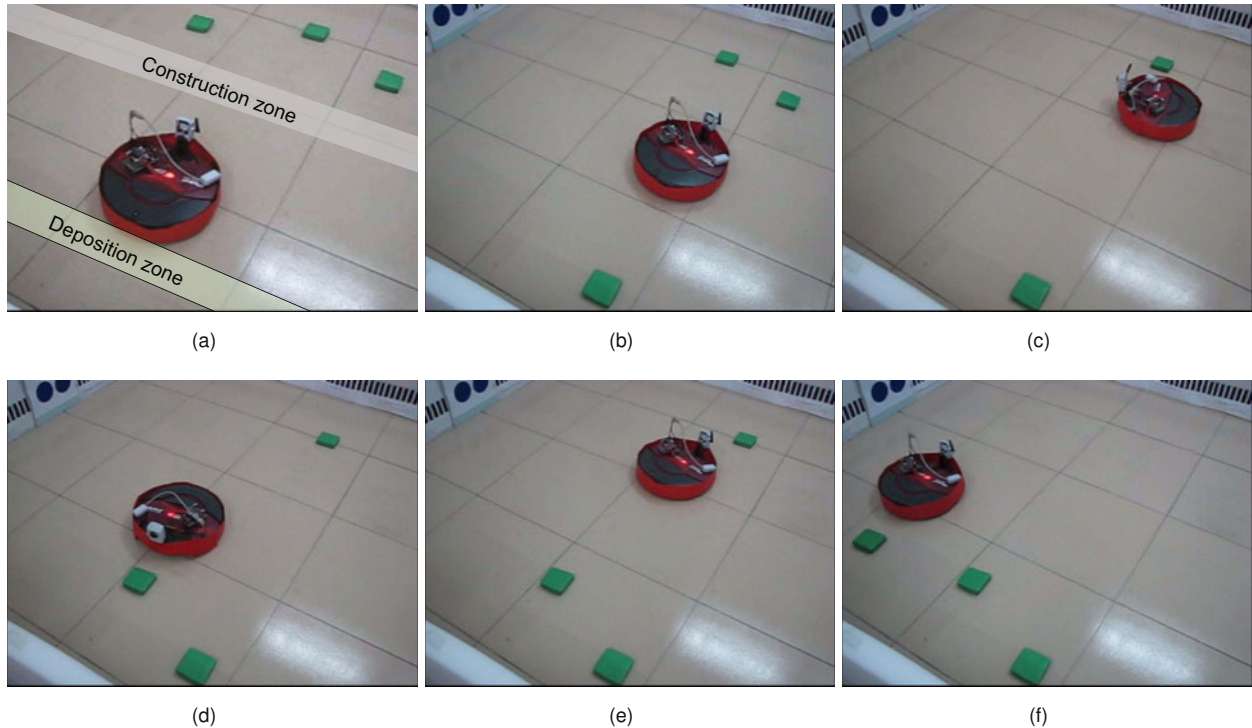


Fig. 13 Linear wall construction with one physical robot ($q_0 = 0.008$, construction time = 443 s). (a) is the initial experimental setup. The beacon is in the top left corner of the picture. The construction zone lies directly in front of the beacon. The deposition zone is parallel to the construction zone. Bricks (cardboard blocks) are placed randomly on one side of the experimental environment. (b)–(f) are snapshots during the construction process. The completion of the construction is defined as robots depositing three bricks within the deposition zone. Due to a large value of q_0 , bricks were not deposited precisely. More details are given in the text

with the simulation results shown in Fig. 12.

7 Conclusions

This research involves the assessment of the feasibility of the proposed visual template mechanism in collective construction. Our main contribution is to demonstrate that as in nature, visual landmarks can be used in the completion of a collective task. Specifically, we applied the visual template mechanism to the task of building a linear wall structure. A behavior-based robot controller was presented for the construction task. Both simulation and physical experiments were conducted. For the simulation part, first, the look-and-turn walking strategy was analyzed with different turning radii, and a desirable turning radius was chosen for the experiments. Then collective construction with different numbers of simulated robots was performed. We found that, by using multiple robots, the wall structure grows

more quickly up until six robots, since the rate of robots entering the construction zone increases with the number of construction robots. Meanwhile, with more robots the possibility of interference increases. This results in the saturation effect which is typical in multi-robot systems. It appears that a performance peak is between six and eight robots in our system.

For the physical experiments, collective construction with iRobot Roomba robots was performed. Results demonstrate that using the visual template mechanism, robots could collectively build the desired structure. The accuracy of construction is limited by the threshold value of q_0 and the precision of the robots' sensors. A decrease in the value of q_0 improves the deposition accuracy and at the same time lengthens the construction time.

Our study has shown that the proposed visual template mechanism works well in collective construction. For our controller to function properly,

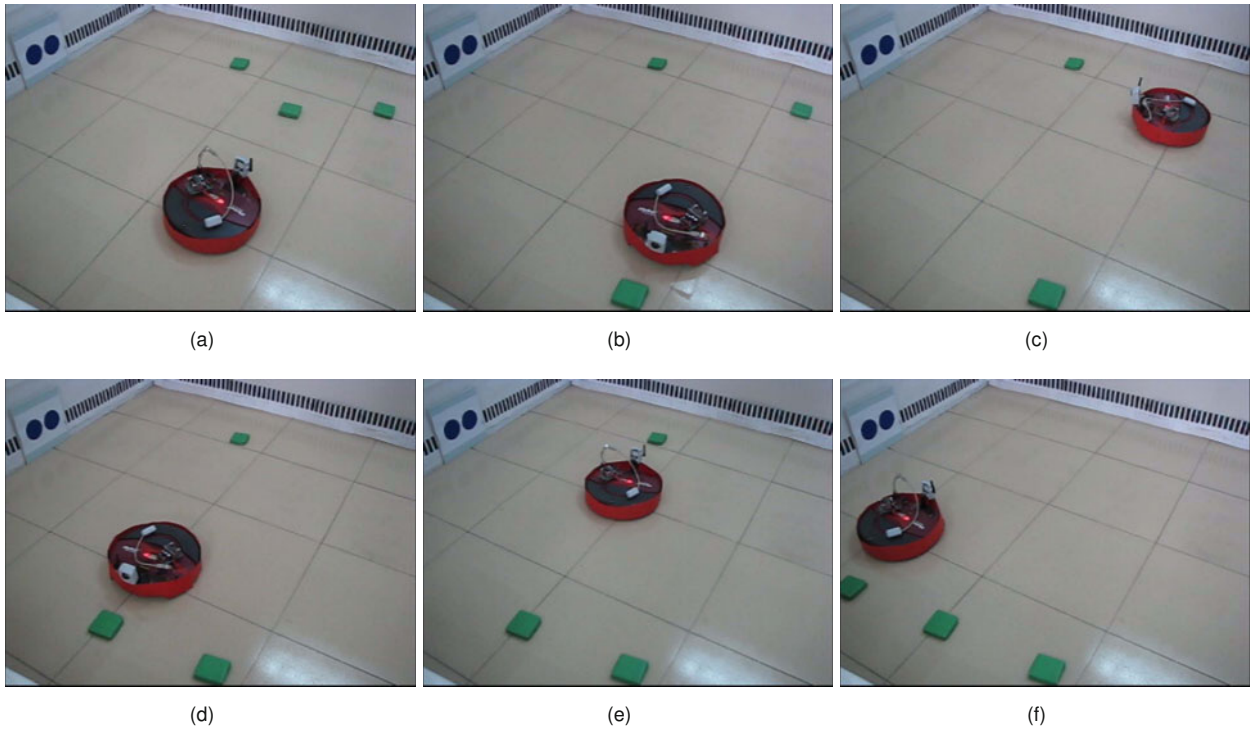


Fig. 14 Linear wall construction with one physical robot ($q_0 = 0.003$, construction time = 586 s). Definitions are the same as in Fig. 13. Since the value of q_0 was smaller than that in Fig. 13, bricks were deposited more accurately. More details are given in the text

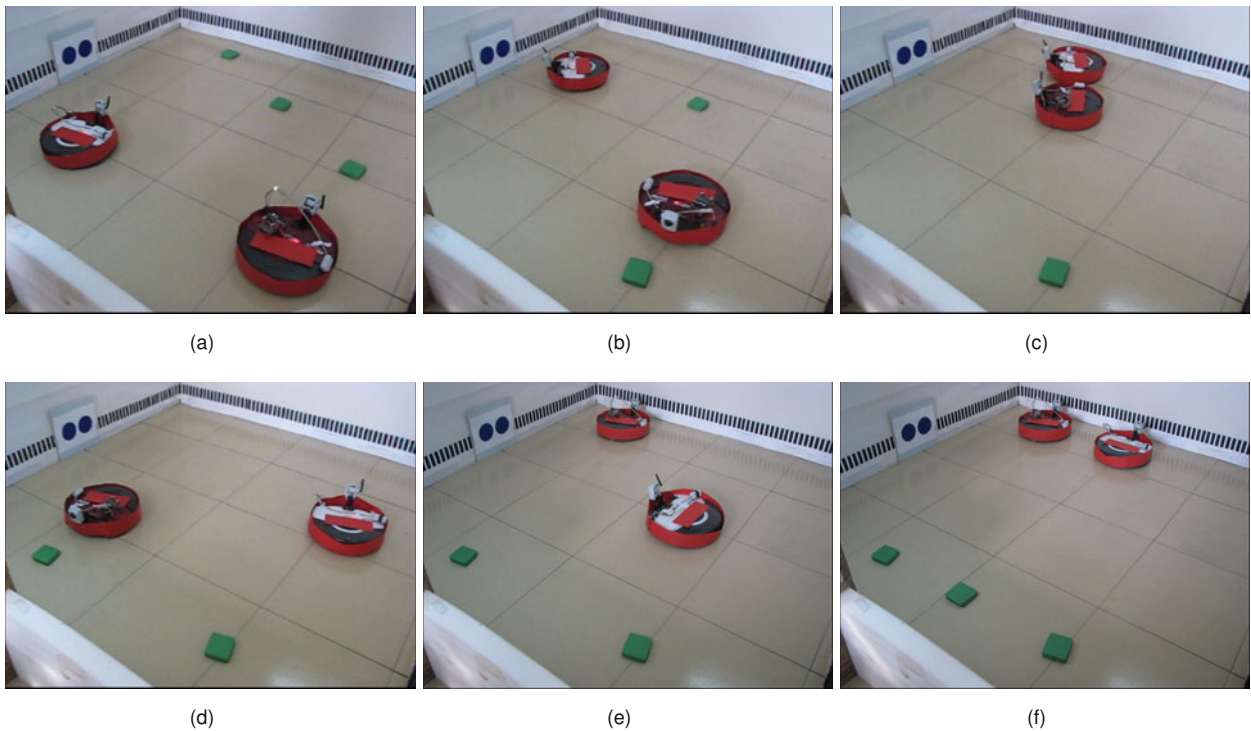


Fig. 15 Linear wall construction with two physical robots ($q_0 = 0.003$, construction time = 338 s). Definitions are the same as in Fig. 13. Since the value of q_0 was equal to that in Fig. 14, similar results were obtained. More details are given in the text

we need to tune certain parameters. In addition, the proposed visual template mechanism allows for robots manipulating homogeneous bricks in a distributed fashion using no direct communication. Although we used a simple visual pattern (two circles) to implement a landmark, robots could use any reference point or salient object in an unknown environment as a landmark. When there are several candidates for the 'final landmark', robots could vote and reach a consensus (Parker and Zhang, 2009) before the construction. The flexibility of selecting a visual landmark allows collective construction in a practical way.

Our future work includes conducting experiments with more physical robots and extending the visual template mechanism to the construction of more complicated structures. We are also interested in experimenting with the selection of natural landmarks as a beacon for collective construction using the collective decision making algorithm (Parker and Zhang, 2009).

Acknowledgements

We thank Robert L. STEWARD and Hai-bo WANG for having commented and having made suggestions on drafts of the paper. We thank Chengyu LIU and Cai-hong LI for helpful suggestions and insights. We thank Xue-wen RONG, Qing-zhi MENG, and Qin-jiang XU for their help with the experiments.

References

- Bayindir, L., Sahin, E., 2009. Modeling Self-Organized Aggregation in Swarm Robotic Systems. *IEEE Swarm Intelligence Symp.*, p.88-95. [doi:10.1109/SIS.2009.4937849]
- Berman, S., Lindsey, Q., Sakar, M.S., Kumar, V., Pratt, S.C., 2011. Experimental study and modeling of group retrieval in ants as an approach to collective transport in swarm robotic systems. *Proc. IEEE*, **99**(9):1470-1481. [doi:10.1109/JPROC.2011.2111450]
- Bonabeau, E., Theraulaz, G., Deneubourg, J., Franks, N.R., Rafelsberger, O., Joly, J., Blanco, S., 1998. A model for the emergence of pillars, walls and royal chambers in termite nests. *Phil. Trans. R. Soc. Lond. B*, **353**(1375):1561-1576. [doi:10.1098/rstb.1998.0310]
- Camazine, S., Franks, N.R., Sneyd, J., Bonabeau, E., Deneubourg, J.L., Theraulaz, G., 2001. *Self-Organization in Biological Systems*. Princeton University Press, Princeton, NJ, USA.
- Collett, T.S., Collett, M., 2002. Memory use in insect visual navigation. *Nat. Rev. Neurosci.*, **3**(7):542-552. [doi:10.1038/nrn872]
- Collett, T.S., Graham, P., Durier, V., 2003. Route learning by insects. *Curr. Opin. Neurobiol.*, **13**(6):718-725. [doi:10.1016/j.conb.2003.10.004]
- Fry, S.N., Wehner, R., 2005. Look and turn: landmark-based goal navigation in honey bees. *J. Exp. Biol.*, **208**(20):3945-3955. [doi:10.1242/jeb.01833]
- Hartley, R.I., Zisserman, A., 2004. *Multiple View Geometry in Computer Vision* (2nd Ed.). Cambridge University Press, Cambridge, UK. [doi:10.1017/CBO9780511811685]
- Kelly, J., Zhang, H., 2006. Combinatorial Optimization of Sensing for Rule-Based Planar Distributed Assembly. *Proc. IEEE/RSJ Int. Conf. on Intelligent Robots and Systems*, p.3728-3734. [doi:10.1109/IROS.2006.281754]
- Kube, C.R., Zhang, H., 1993. Collective robotics: from social insects to robots. *Adapt. Behav.*, **2**(2):189-218. [doi:10.1177/105971239300200204]
- Kube, C.R., Parker, C.A., Wang, T., Zhang, H., 2005. Biologically Inspired Collective Robotics. *In: de Castro, L.N., von Zuben, F.J. (Eds.), Recent Developments in Biologically Inspired Computing*. Idea Group Publishing, New York, p.369-397.
- Ladley, D., Bullock, S., 2005. The role of logistic constraints in termite construction of chambers and tunnels. *J. Theor. Biol.*, **234**(4):551-564. [doi:10.1016/j.jtbi.2004.12.012]
- Melhuish, C., Welsby, J., Edwards, C., 1999. Using Templates for Defensive Wall Building with Autonomous Mobile Ant-like Robots. *Proc. Towards Intelligent Mobile Robots*.
- Parker, C.A.C., Zhang, H., 2006. Collective robotic site preparation. *Adapt. Behav.*, **14**(1):5-19. [doi:10.1177/105971230601400101]
- Parker, C.A.C., Zhang, H., 2009. Cooperative decision-making in decentralized multiple-robot systems: the best-of-*n* problem. *IEEE/ASME Trans. Mechatron.*, **14**(2):240-251. [doi:10.1109/TMECH.2009.2014370]
- Parker, C.A.C., Zhang, H., 2011. Biologically inspired collective comparisons by robotic swarms. *Int. J. Robot. Res.*, **30**(5):524-535. [doi:10.1177/0278364910397621]
- Parker, C.A.C., Zhang, H., Kube, C.R., 2003. Blind Bulldozing: Multiple Robot Nest Construction. *Proc. IEEE/RSJ Int. Conf. on Intelligent Robots and Systems*, **2**:2010-2015.
- Payton, D., Estkowski, R., Howard, M., 2005. Pheromone Robotics and the Logic of Virtual Pheromones. *In: Sahin, E., Spears, W. (Eds.), Swarm Robotics*. Springer Berlin/Heidelberg, p.45-57.
- Purnamadajaja, A.H., Russell, R.A., 2010. Bi-directional pheromone communication between robots. *Robotica*, **28**(1):69-79. [doi:10.1017/S0263574709005591]
- Skibniewski, M., 2000. New Directions and Developments in Robotics and Site Automation in the U.S.A. *Proc. 17th ISARC*, p.k3-k14.
- Stewart, R.L., Russell, R.A., 2006. A distributed feedback mechanism to regulate wall construction by a robotic swarm. *Adapt. Behav.*, **14**(1):21-51. [doi:10.1177/105971230601400104]
- Terada, Y., Murata, S., 2004. Automatic Assembly System for a Large-Scale Modular Structure—Hardware Design of Module and Assembler Robot. *Proc. IEEE/RSJ Int. Conf. on Intelligent Robots and Systems*, **3**:2349-2355.

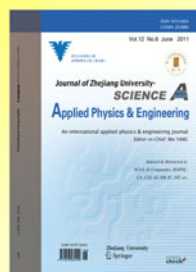
- Theraulaz, G., Bonabeau, E., Deneubourg, J.L., 1998. The origin of nest complexity in social insects. *Complexity*, **3**(6):15-25. [doi:10.1002/(SICI)1099-0526(199807/08)3:6<15::AID-CPLX3>3.3.CO;2-M]
- Theraulaz, G., Gautrais, J., Camazine, S., Deneubourg, J.L., 2003. The formation of spatial patterns in social insects: from simple behaviours to complex structures. *Phil. Trans. R. Soc. Lond. A*, **361**(1807):1263-1282. [doi:10.1098/rsta.2003.1198]
- Wawerla, J., Sukhatme, G.S., Mataric, M.J., 2002. Collective Construction with Multiple Robots. Proc. IEEE/RSJ Int. Conf. on Intelligent Robots and Systems, **3**:2696-2701. [doi:10.1109/IRDS.2002.1041677]
- Werfel, J., Nagpal, R., 2008. Three-dimensional construction with mobile robots and modular blocks. *Int. J. Robot. Res.*, **27**(3-4):463-479. [doi:10.1177/0278364907084984]
- Werfel, J., Bar-Yam, Y., Rus, D., Nagpal, R., 2006. Distributed Construction by Mobile Robots with Enhanced Building Blocks. Proc. IEEE Int. Conf. on Robotics and Automation, p.2787-2794. [doi:10.1109/ROBOT.2006.1642123]

Recommended reading

- Werfel, J., Ingber, D.E., Nagpal, R., 2007. Collective Construction of Environmentally-Adaptive Structures. Proc. IEEE/RSJ Int. Conf. on Intelligent Robots and Systems, p.2345-2352.
- Werfel, J., Nagpal, R., 2008. Three-dimensional construction with mobile robots and modular blocks. *Int. J. Robot. Res.*, **27**(3-4):463-479. [doi:10.1177/0278364907084984]
- Kelly, J., Zhang, H., 2006. Combinatorial Optimization of Sensing for Rule-Based Planar Distributed Assembly. Proc. IEEE/RSJ Int. Conf. on Intelligent Robots and Systems, p.3728-3734. [doi:10.1109/IROS.2006.281754]
- Petersen, K., Nagpal, R., Werfel, J., 2011. TERMES: an Autonomous Robotic System for Three-Dimensional Collective Construction. Proc. Robotics: Science and Systems.
- Bonabeau, E., Theraulaz, G., Deneubourg, J., Franks, N.R., Rafelsberger, O., Joly, J., Blanco, S., 1998. A model for the emergence of pillars, walls and royal chambers in termite nests. *Phil. Trans. R. Soc. Lond. B*, **353**(1375):1561-1576. [doi:10.1098/rstb.1998.0310]

Accepted manuscript available online (unedited version)

<http://www.zju.edu.cn/jzus/inpress.htm>



JZUS-A
(Applied Physics & Engineering)



JZUS-B
(Biomedicine & Biotechnology)



JZUS-C
(Computers & Electronics)

- As a service to our readers and authors, we are providing the unedited version of accepted manuscripts.
- The section "Articles in Press" contains peer-reviewed, accepted articles to be published in *JZUS (A/B/C)*. When the article is published in *JZUS (A/B/C)*, it will be removed from this section and appear in the published journal issue.
- Please note that although "Articles in Press" do not have all bibliographic details available yet, they can already be cited as follows: Author(s), Article Title, Journal (Year), DOI. For example:
ZHANG, S.Y., WANG, Q.F., WAN, R., XIE, S.G. Changes in bacterial community of anthracene bioremediation in municipal solid waste composting soil. *J. Zhejiang Univ.-Sci. B (Biomed. & Biotechnol.)*, in press (2011). [doi:10.1631/jzus.B1000440]
- Readers can also give comments (Debate/Discuss/Question/Opinion) on their interested articles in press.